Electrostatic Droplet Generation: Mechanism of Polymer Droplet Formation

Branko Bugarski, Qiangliang Li, and Mattheus F. A. Goosen
Dept. of Chemical Engineering, Queen's University, Kingston, Ontario K7L 3N6, Canada

Denis Poncelet and Ronald J. Neufeld
Dept. of Chemical Engineering, McGill University, Quebec, Canada

Gordana Vunjak
Dept. of Chemical Engineering, Massachusetts Institute of Technology, Cambridge, MA 02139

The mechanism of alginate droplet formation and experimental parameters for producing very small polymer microbeads (less than 100 μm dia.) using an electrostatic droplet generator studied showed that the microbead size was a function of needle diameter, charge arrangement (electrode geometry and spacing) and strength of electric field. Perfectly spherical and uniform polymer beads, 170 μm dia., for example, were obtained at a potential difference of 6 kV with a 26-gauge needle and an electrode distance of 2.5 cm. Increasing the electric field, and thus the surface charge in the vicinity of the needle, by increasing the applied potential, resulted in needle oscillation, giving a bimodal bead size distribution with a large fraction (30–40%) of microbeads with a mean diameter of 50 μm. The process of alginate droplet formation under the influence of electrostatic forces assessed with an image analysis/video system revealed distinct stages. After a voltage was applied, the liquid meniscus at the needle tip was distorted from a spherical shape into an inverted cone-like shape. Consequently, alginate solution flowed into this cone at an increasing rate causing formation of a neck-like filament. When this filament broke away, producing small droplets, the meniscus relaxed back to a spherical shape until flow of the polymer caused the process to start again. A large-scale multineedle device with a processing capacity of 0.7 L/h was also designed and produced uniform 400 ± 150 μm microbeads.

Introduction

Electrostatic atomization and electrostatically assisted atomization have been employed in a variety of areas, including paint spraying (Balachandran and Baily, 1982), electrostatic printing (Fillimore, 1982), and cell immobilization (Keshavarz et al., 1992). The basic concept behind these applications involves electrostatic forces which work to disrupt a liquid surface to form a charged stream of fine droplets. The effect of electrostatic forces on mechanically atomized liquid droplets was first studied in detail by Lord Rayleigh (1882, 1945) who investigated the hydrodynamic stability of a jet of liquid with and without an applied electric field.

When a liquid is subjected to an electric field, a charge is induced on the surface of the liquid. Mutual charge repulsion results in an outwardly directed force. Under suitable conditions, for example, extrusion of a liquid through a needle, the electrostatic pressure at the surface forces the liquid drop into a cone shape. Surplus charge is ejected by the emission of charged droplets from the tip of the liquid. The emission process depends on such factors as the needle diameter, distance from the collecting solution, and applied voltage (strength of electrostatic field) (Nawab and Mason, 1958). Under most circumstances, the electrical spraying process is random and irregular, resulting in drops of varying size and charge that are emitted from the capillary tip over a wide range of angles.

Correspondence concerning this article should be addressed to M. F. A. Goosen.

However, when the electrostatic generator configuration has been adjusted for liquid pressure, applied voltage, electrode spacing, and charge polarity, the spraying process can become quite regular and periodic.

A major concern in cell and bioactive agent immobilization has been the production of very small microbeads so as to minimize the mass-transfer resistance problem associated with large-diameter beads (> 1,000 μm) (Fonseca et al., 1986). Klien et al. (1983) reported production of alginate beads with diameters from 100 to 400 μm using compressed air to quickly pass the cell/gel solution through a nozzle. Surprisingly, few attempts have been made in the application of electric fields to the production of micron-size polymer beads for cell immobilization (Goosen et al., 1986).

The primary objective of this article was to investigate the mechanism of droplet formation as well as the experimental parameters which are critical for producing very small polymer microbeads (< 100 μm dia.) using an electrostatic droplet generator. Parameters such as applied voltage, needle size, polymer concentration, and electrode spacing and geometry were assessed. The study was limited to two cases where a positively charged vertically mounted needle and a parallel plate electrode setup were used to extrude alginate solutions at a low constant flow rate. Video and image analysis were performed to reveal details of the mechanism of droplet formation under the influence of an electrostatic field. Furthermore, animal cell suspensions were also extruded using the electrostatic droplet generator to investigate the application of this technology to cell immobilization.

Experimental Studies

Droplet formation using electrostatic droplet generation

Spherical droplets were formed with a syringe pump (Razel, Scientific Instruments, Stamford, CT)/electrostatic droplet generator which extruded the polymer through a 22 or 26 gauge needle (H80763, H80429, Chromatographic Specialties Inc., Brockville, Canada). As the liquid was forced out of the end of the needle by the syringe pump (0.036 L/h), the droplets were pulled off by the action of gravitational and electrostatic forces. The needle tip was mounted 2.5, 3.5, and 4.8 cm above the 1.5% $CaCl_2$ hardening solution (BDH, Toronto, Canada). The potential difference was controlled with a voltage power supply (Model 30R, Bertan Associates, Inc., New York) with a maximum current of 0.4 mA and variable voltage of 0 to 30 kV.

Our investigation was focused on the interaction between charge polarity arrangement, polymer concentration, electrode spacing/geometry, and needle size on average bead diameter. Three types of experiments were carried out to determine the optimum conditions for the production of small polymer beads. In the first setup, a parallel-plate electrode system was employed to produce a uniform electric field in the same direction as that of gravity. The upper electrode was brought to a positive potential and the polymer droplets were formed at a 90° blunt needle protruding through a small aperture at the center of the disk electrode. The grounded plate with a hardening solution ($CaCl_2$) had the same dimensions as the upper charged plate.

In the second type of experiment, the effect of a point to plane charge on droplet formation was examined. The production of charged polymer beads was accomplished by establishing an electric field between a positively charged needle and grounded plate containing 1.5% $CaCl_2$ hardening solution.

Finally, for scaleup purposes a 1.5-L cylindrical reservoir (15 cm height by 10 cm dia.) containing 20 needles for the continuous production of polymer beads was designed. The liquid flow rate was kept constant at 0.7 L/h (36 mL/h per needle) by adjusting the air pressure head above the polymer solution. A ground collecting plate of $CaCl_2$ solution was placed 2.5 cm below the needles. The 20 (22 gauge) stainless steel needles, 1.2 cm radially apart, were connected to the cylindrical reservoir containing 1 L of polymer solution and then attached to the high potential unit.

Analysis of droplet formation using image analysis

Droplet formation under the influence of electrostatic forces was examined with a stroboscopic light (Strobotac, GRC, MA) at a defined frequency (50–400/s) along with a video/image analysis system. Images were recorded when the frequencies of light and the forming bead were identical so that the object appeared to be frozen. The image analysis system consisted of several components: a video camera (Panasonic Digital 5100), a Sony CC camera (model AAVCD5), a video adapter (Sony, CMAD5, Sony, Japan), a video monitor (Sony Trinitron, PVM1342Q), a VHS recorder (NV-8950, Panasonic, Japan), a PC (486), and software Java (ver. 1.3) for image analysis (Jandel Scientific, CA, USA). For closeup studies of droplet formation, the video camera was connected to a microscope lens (Olympus SZH, Optical Co. Ltd., Japan).

A sample of microbeads containing 50 to 150 beads was taken from each set of extrusion experiments. The diameter of individual beads was measured under the microscope using the image analysis program. The average diameter of the beads and standard deviation with the maximum and minimum from each set were computed automatically.

Determination of microbead size distribution by laser light scattering

Volumetric (volume of microspheres in each diameter class) and cumulative size distribution were determined by laser light scattering, with a 2602-LC particle analyzer (Malverin Instruments) according to the log-normal distribution model. The mean diameter and the arithmetic standard deviation were calculated from the cumulative distribution curve (Poncelet, 1989).

Extrusion of an animal cell suspension using the electrostatic droplet generator

Animal cell sensitivity to a high potential (6–8 kV) was examined by extruding an insect cell (SF-9) suspension using a positively charged 26-gauge needle setup. The cell viability was assessed by staining the cells with trypan blue dye (only live cells can exclude the dye from the cell nucleus). The cells were cultured in shake flasks in IPL41 medium prior to extrusion.

Results and Discussion

Investigation of parameters affecting microbead size

In the case of the positively charged needle setup, the effect

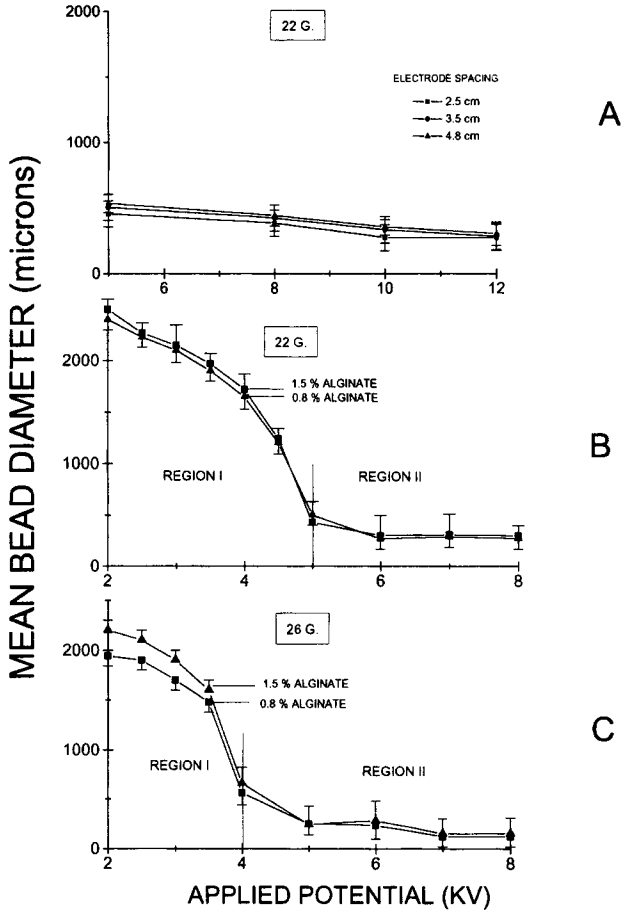

Figure 1. Effect on microbead size: A. applied potential and electrode spacing; B. alginate concentration; and C. needle size with the positively charged needle setup.

A 22-gauge needle was used in A and B and a 26-gauge needle in C.

of electrode spacing on alginate bead size, produced with a 22-gauge needle, is shown in Figure 1A. The electrode spacing was not found to be significant over the range investigated. For example, at an applied voltage of 6 kV, the mean bead size decreased from 530 to 450 μm, as the electrode spacing decreased from 4.8 to 2.5 cm, respectively, with a standard deviation of approximately 100 μm. When the applied voltage to the alginate solution was increased to 12 kV, at a distance between the needle tip and collecting solution of 4.8 cm, the average bead diameter decreased to 340 μm. Keeping the applied potential constant at 12 kV, but reducing the electrode distance to 2.5 cm, resulted in only a slightly smaller bead size (300 μm).

The relationship between the applied voltage, alginate concentration, and droplet diameter was also investigated (Figures 1B and 1C). When the alginate concentration was decreased from 1.5 to 0.8% the average bead diameter decreased 10 to 20%. The standard deviation also decreased at the lower polymer concentration due to a more uniform bead size distribution. For example, at an applied voltage of 5 kV, the mean bead diameter decreased from 440 to 380 μm with standard deviations of ± 200 and ± 80 μm for microbeads prepared with alginate concentrations of 1.5 and 0.8%, respectively.

While the alginate concentration was not found to be significant, bead diameter could be readily controlled by needle size and applied voltage (Figures 1B and 1C). For example, at an applied voltage of 4 kV, the mean bead diameter was reduced by a factor of 3 from approximately 1,700 to 600 μm when the needle size was reduced from 22 to 26 gauge. In the case of the 26-gauge needle, as the voltage increased above 6 kV, natural harmonic oscillation of the needle was observed. This resulted in formation of microbeads, a large fraction of which were 50 μm in diameter.

A recent study of a similar electrostatic method for alginate bead formation (Keshavarz et al., 1992) showed that with a 23-gauge needle the minimum alginate bead size achievable varied between 600 and 1,000 μm when 5 kV was applied to the capillary tip. In our study, with the same voltage and a slightly larger needle (22 gauge) it was shown that it is possible to achieve a bead diameter 50% smaller than that reported by Keshavarz. This difference may be partly due to a higher alginate concentration (2%, Keshavarz et al., 1992) compared to a 1.5% alginate solution used in our study. With a 26-gauge needle under the same conditions, the bead diameter in our studies decreased further, to about 170 ± 100 μm, suggesting a strong influence of needle size on bead diameter.

Effect of electrode geometry on microbead size

In the case of the parallel plate setup, the effect of electrode spacing and charge arrangement (different electric field and surface charge intensity) on polymer bead size is shown in Figure 2A. As the potential between the electrodes in the parallel plate setup, for example, increased from 6 to 12 kV at 4.8 cm, the average bead diameter decreased from 2,300 to 700 μm using a 22-gauge needle. Reducing the electrode distance resulted in even smaller bead sizes, suggesting a strong influence of distance and voltage on microbead size with this charge arrangement. For example, at 10 kV, reducing the distance from 4.8 to 2.5 cm resulted in a decrease in polymer bead diameter from 1,500 to 350 μm. Increasing the applied potential above 12 kV and decreasing the electrode spacing did not result in smaller bead diameters. This was probably due to a discharge between the plates accompanied by sparking as a result of air ionization in the space between the electrodes.

For a fixed electrode distance (2.5 cm), needle length (1.3 cm), and alginate concentration (1.5%), the bead diameter could be reduced by decreasing the needle size from 22 to 26 gauge (Figure 2B). A decrease by a factor of 2 in bead diameter was observed over a wide range of applied potential (2–8 kV).

The multiple needle device was essentially a scaled-up version of the parallel plate setup, which is similar to that found with the single-needle setup. At an electrode distance of 2.5 cm, increasing the potential from 7 to 12 kV resulted in a decrease in bead diameter from 950 ± 100 μm to 400 ± 150 μm (Figure 2C). The 20-needle device for the continuous production of beads had a processing capacity of 0.7 L/h.

Investigation of mechanism of droplet formation with the image analysis/video system

In the absence of an electrostatic field with gravitational force acting alone, the mean bead diameter was $2,400 \pm 200$ μm at a constant alginate flow rate of 36 cm^3/h and using a 22-gauge needle. In this case, a droplet was produced every 1

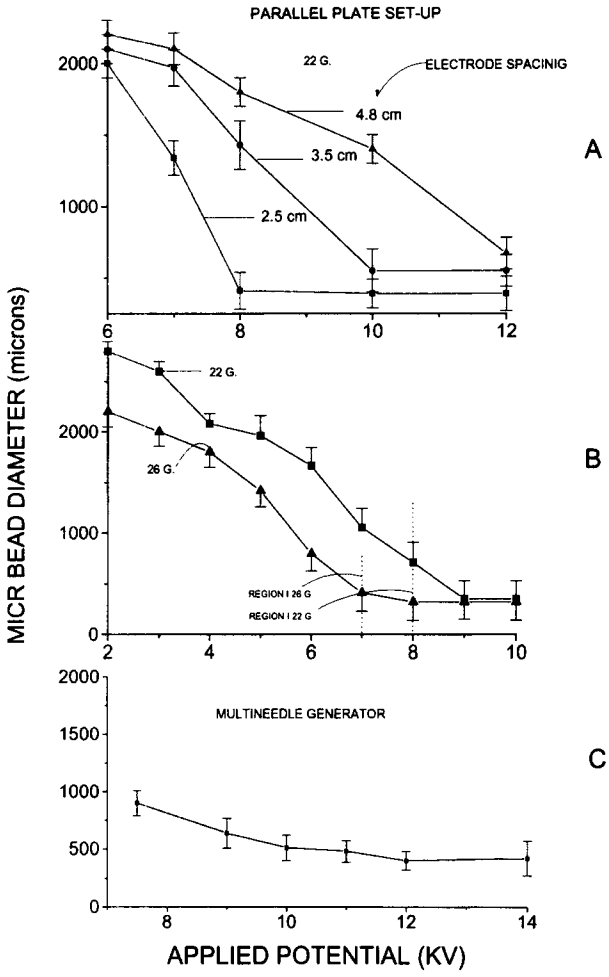

Figure 2. Effect on microbead diameter: A. applied potential and electrode spacing; B. needle size; and C. scaleup with a parallel plate setup.

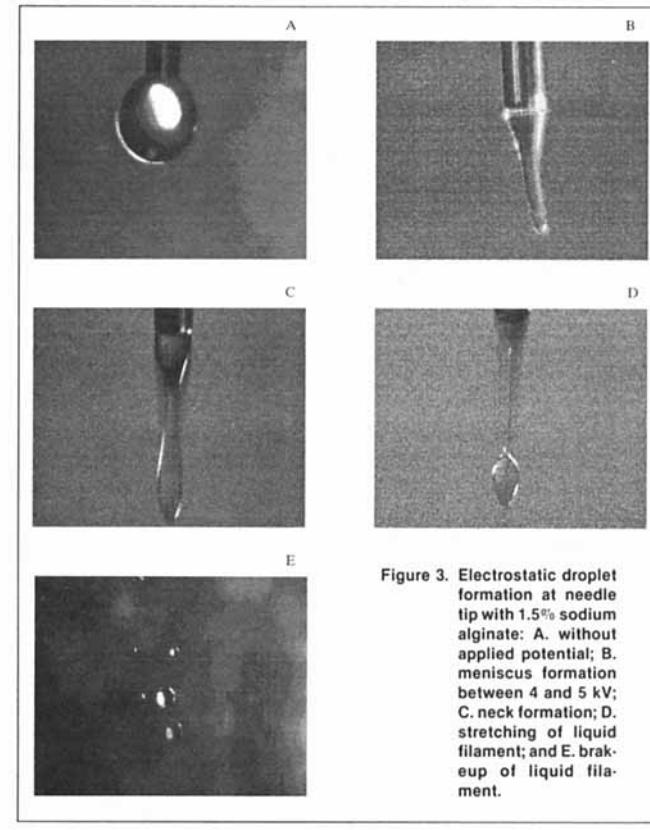

Figure 3. Electrostatic droplet formation at needle tip with 1.5% sodium alginate: A. without applied potential; B. meniscus formation between 4 and 5 kV; C. neck formation; D. stretching of liquid filament; and E. brakeup of liquid filament.

to 2 s. Each drop grew at the tip of the needle until its weight overcame the net vertical component of the surface tension force (Figure 3A).

Examination of the formation of droplets under the influence of electrostatic forces revealed that an elongated cone formed as the droplet meniscus advanced (Figure 3B). The forming droplet was drawn out into a long, slender filament (4–5 kV, 2.5 cm electrode distance, 1.5% sodium alginate concentration, flow rate of 36 cm^3/h, 22-gauge needle). A high charge density at the tip of the inverted cone reduced the surface tension of the alginate solution (Hendricks, 1964) resulting in neck formation (Figure 3C). For the more concentrated alginate (1.5%), the neck elongated up to 1 mm before detachment (Figure 3D). While the main part of the liquid neck quickly coalesced into a new drop, the long linking filament broke up into a large number of smaller drops (Figure 3E). It was also observed that small (satellite) droplet formation usually accompanied higher voltages (above 6 kV), because the elongation of the liquid neck prior to rupture was much more pronounced. The largest of these drops was one half of the main drop diameter, while the smallest was less than 20 μm.

When the alginate concentration was decreased from 1.5 to 0.8%, a difference was observed in the formation of the long, thin neck or a filament linking the new droplet and the meniscus at the tip of the needle. For the low-viscosity alginate, neck elongation was not as pronounced, resulting in a more uniform bead size.

When the voltage was increased above 6 kV, harmonic natural needle oscillation was observed, but only with the thinner and lighter 26-gauge needle. A high surface charge and an electric field on the surface of capillary tip gave rise to a mechanical force causing needle vibration and resulting in an oscillating thread-like filament. The periodic oscillation of the electrically stressed meniscus at the capillary tip caused a sinusoidal shaped filament to detach from the needle tip. The long tapered filaments were formed as a result of the surface energy component arising from the presence of the surface charge (Bugarski, 1993, unpublished data). From a consideration of the minimum surface energy, molecular forces tend to decrease the surface to volume ratio, whereas the energy component due to electrostatic charges is minimized by increasing this ratio. Figure 4A indicates the manner in which the stream disintegrates by a vigorous whipping action. Fragmentation of the filament results in a bimodal size distribution with peaks at 50 and 190 μm in dia. (Figure 5C). This phenomenon was not observed with a 22-gauge needle.

A comparative analysis of the two charge setups at the same applied potential and needle size was carried out to give insight into the droplet formation mechanism. It was observed that each charge setup produced a different mode of droplet formation. At the same relatively high potential difference (6 kV), needle size (26 gauge), electrode spacing (2.5 cm), and flow rate (36 mL/h), there was a noticeable difference in bead di-

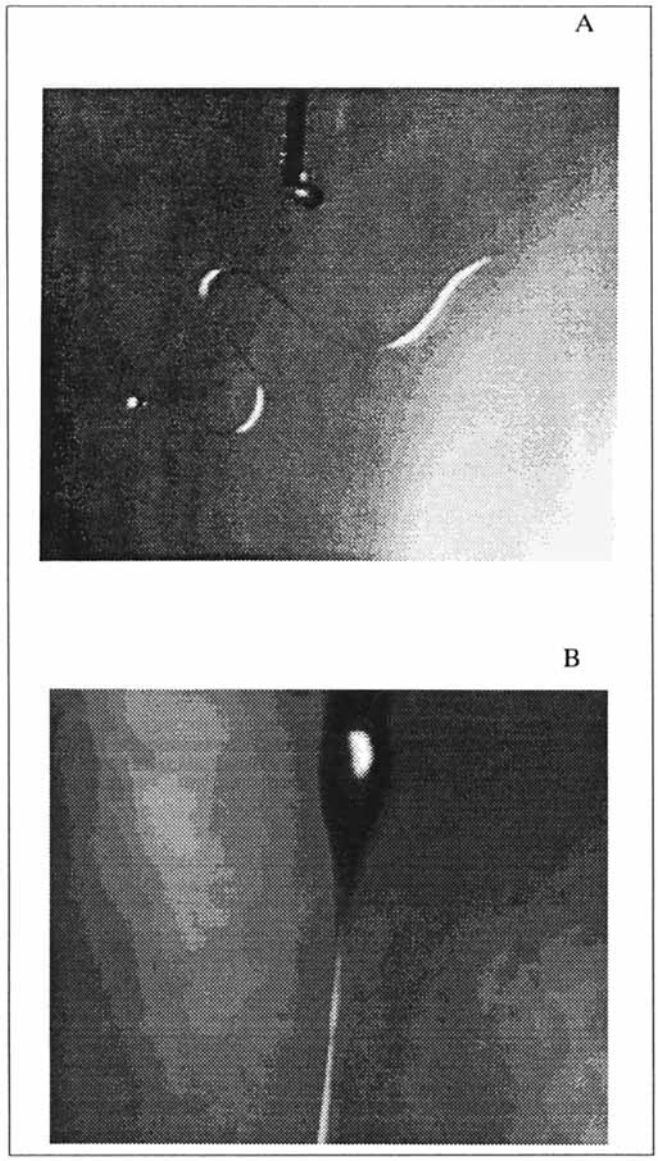

Figure 4. A. Needle oscillation (26 gauge, 7 kV) due to electrostatic forces and detachment of liquid filament; B. Taylor cone-like meniscus with well developed jet (26 gauge, 6 kV, 2.5 cm).

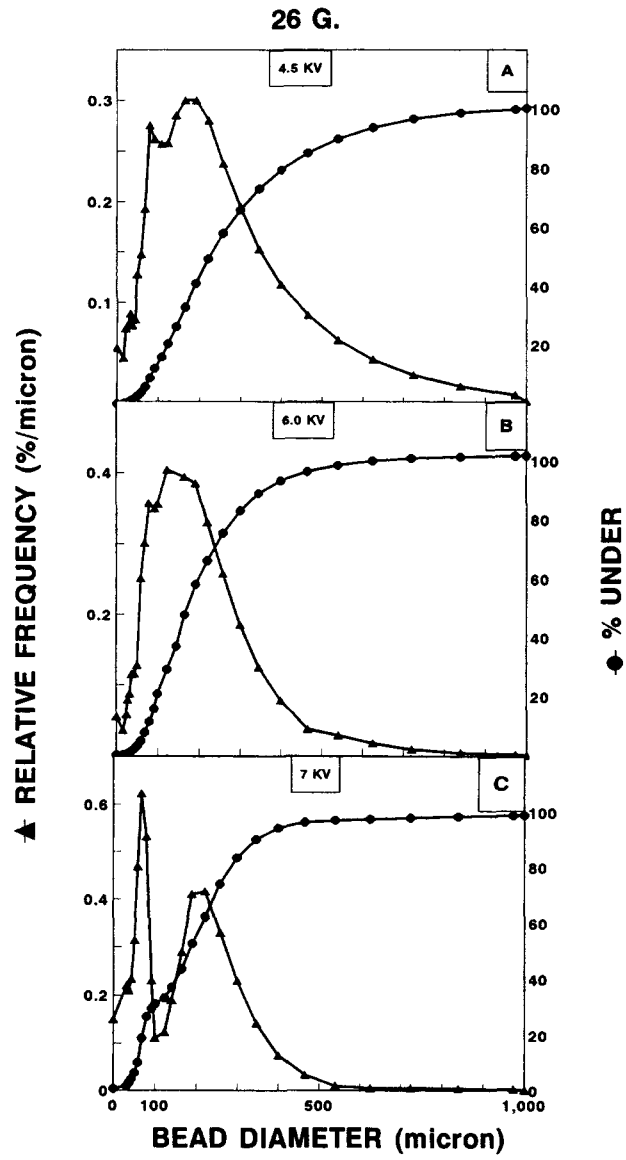

Figure 5. Droplet size distribution produced with positively charged 26-gauge needle, 2.5 cm electrode distance, and 0.8% alginate concentration: A. 4.5 kV; B. 6 kV, and C. 7 kV.

ameter. With the parallel plate charge setup, for example, the average bead diameter was found to be $1,100 \pm 200$ μm. In contrast, with the positively charged needle, a Taylor cone-like meniscus (Taylor, 1966) was observed with a well developed jet (80 μm dia.) ejecting droplets of 170 ± 70 μm in dia. (Figure 4B), a decrease by factor 7.

Microbead size distribution

The mean bead size distribution curves obtained by plotting relative frequencies vs. bead diameter typically resulted in a continuous function symmetrical about the mean value. At 4.5 and 6 kV, the mean bead size distribution was found to vary about the mean of 225 μm (Figure 5A) and 170 μm (Figure 5B), respectively. However, in the case of the naturally vibrating needle (7 kV), a bimodal bead size distribution was observed, one peak at 50 μm and the second peak at 190 μm (Figure 5C).

Effect of electrostatic droplet generation on cell viability

To assess the effect of an electrostatic field on animal cell viability, an insect cell suspension was extruded using the electrostatic droplet generator. No detectable change in insect cell viability was observed after extrusion. The initial cell density, 4×10^5 cell/mL, remained essentially unchanged at 3.85×10^5 and 3.8×10^5 cell/mL immediately after passing through the generator at an applied potential difference of 6 and 8 kV, respectively. Prolonged cultivation of these cells did not show any loss of cell density or viability (Table 1).

Table 1. Effect of Electrostatic Droplet Generator on Animal Cell Viability*

Time (d)	Density (Cells/mL) $\times 10^{-5}$	Cell Viability (%)
0	4	100
0**	3.8	93
2	7.5	90
4	10	94
6	13	92

* Growth in suspension after extrusion with electrostatic voltage generator at 8 kV potential difference with positively charged needle.
** Immediately after application of high voltage.

Conclusions

The formation of droplets with a charged needle and a parallel plate arrangement in a defined electric field was examined. In the parallel plate setup, reducing the electrode distance and increasing the applied voltage resulted in smaller beads, suggesting a strong influence of distance and applied potential on bead diameter. Further reduction in bead size with both setups was achieved by decreasing the needle size. Electrode spacing was not important with the positively charged needle arrangement. The greatest decrease in microbead size was observed when natural needle oscillation, caused by surface charge and a high electric field in the vicinity of the needle, resulted in whip-like liquid filaments breaking off the end of the needle. This produced a bimodal size distribution with a large fraction of droplets below 50 μm dia. Modification of the parallel plate setup system in the form of a multineedle device showed that it was possible to continuously produce uniform microbeads at a high processing capacity. Finally, there was no detectable loss in viability after passing animal cells through the electrostatic droplet generator. This is a promising result as it proves the technique amenable for cell immobilization.

Acknowledgment

This work has been funded by a Grant from the Natural Sciences and Engineering Research Council of Canada and the Canada ASEAN Centre.

Literature Cited

Balachandran, W., and A. G. Bailey, "The Dispersion of Liquids Using Centrifugal and Electrostatic Forces," *IEEE Meeting of the Industrial Application Society*, 971 (1982).

Fillimore, G. L., and D. C. Van Lokeren, "Multinozzle Drop Generator Which Produces Uniform Break-up of Continuous Jets," *IEEE Meeting of the Industrial Society*, 991 (1982).

Fonseca, M. M., G. M. Black, and C. Webb, "Reactor Configuration For Immobilized Cells," *Process Engineering Aspects of Immobilized Cell System*, The Institution of Chemical Engineers, England, 63 (1986).

Goosen, M. F. A., G. M. O'Shea, M. M. Gharapetian, and A. M. Sun, "Immobilization of Living Cells in Biocompatible Semipermeable Microcapsules: Biomedical and Potential Biochemical Engineering Applications," *Polymers in Medicine*, E. Chiellini, ed., Plenum Publishing, New York, 235 (1986).

Hendricks, C. D., Jr., "Charged Droplet Experiments," *J. Colloid. Sci.*, **17**, 249 (1964).

Keshavarz, T., G. Ramsden, P. Phillips, P. Mussenden, and C. Bucke, "Application of Electric Field for Production of Immobilized Biocatalysts," *Biotech. Technique*, **6**, 445 (1992).

Klein, J., J. Stock, and D. K. Vorlop, "Pore Size and Properties of Spherical Calcium Alginate Biocatalysts," *Eur. J. Appl. Microbiol. Biotechnol.*, **18**, 86 (1983).

Newab, M. A., and S. G. Mason, "The Preparation of Uniform Emulsions by Electrical Dispersion," *J. Colloid. Sci.*, **13**, 179 (1958).

Poncelet, B., D. Poncelet, and R. J. Neufeld, "Control and Mean Diameter and Size Distribution During Formulation of Microcapsules with Cellulose Nitrate Membranes," *Enzyme Microb. Technol.*, **11**, 29 (1989).

Rayleigh, Lord, *The Theory of Sound*, Vol. II, Dover Publications, New York, p. 372 (1945).

Rayleigh, Lord, "On the Equilibrium of Liquid Conducting Masses Charged with Electricity," *Phil. Mag.*, **14**, 184 (1882).

Taylor, G. I., "The Force Exerted by an Electric Field on Long Cylindrical Conductors," *Proc. R. Soc. A*, **291**, 145 (1966).

Manuscript received June 8, 1993, and revision received Aug. 26, 1993.